Enhanced mechanical strength and conductivity of PVFM based membrane and its supporting polymer electrolytes

Xiao-rong Pan, Fang Lian, Yi He, Yi-fei Peng, Xiao-meng Sun, Yan Wen, Hong-yan Guan

School of Materials Science and Engineering, University of Science and Technology Beijing, Beijing 100083, China
Correspondence to: F. Lian (E-mail: lianfang@mater.ustb.edu.cn)

ABSTRACT: Polyvinyl formal based polymer electrolyte membranes are prepared via the optimized phase inversion method with poly(ethylene oxide) (PEO) blending. The physical properties of blend membranes and the electrochemical properties of corresponding gel polymer electrolytes (GPEs) are characterized by field emission scanning electron microscopy, X-ray diffraction, differential scanning calorimetry, mechanical strength test, electrolyte uptake test, AC impedance spectroscopy, cyclic voltammetry, and galvanostatic charge–discharge test. The comparative study shows that the appearance of PEO obviously enhances the tensile strength of membranes and the ionic conductivity of corresponding GPEs. When the weight ratio of PEO is 30%, the tensile strength of membrane achieves 12.81 MPa, and its GPE shows high ionic conductivity of 2.20×10^{-3} S cm^{-1}, wide electrochemical stable window of 1.9–5.7 V (vs. Li/Li$^+$), and good compatibility with LiFePO$_4$ electrode. © 2015 Wiley Periodicals, Inc. J. Appl. Polym. Sci. **2015**, *132*, 41839.

INTRODUCTION

The rechargeable lithium ion batteries are one of the most promising power sources for electric vehicles due to their high energy density.[1] However, there are still potential safety issues in the commercial lithium ion batteries arising from leakage and combustion of organic electrolytes.[2] The application of GPEs is one of the effective ways to solve the safety issues because of the absence of risk for leakage of electrolytes.[3–5] In recent years, many kinds of polymer matrixes have been researched, including poly(ethylene oxide) (PEO),[6] poly(acrylonitrile) (PAN),[7] poly(methyl methacrylate) (PMMA),[8] poly (vinylidene fluoride) (PVDF),[9] and poly (vinylidene fluoride-hexafluoro propylene) (PVDF-HFP),[10] and so on. Besides, several new kinds of polymer matrixes are being developed for superior electrochemical properties.

In our previous studies, a novel polyvinyl formal (PVFM) based membrane has been prepared successfully via phase inversion method.[11] In detail, the obtained porous membrane shows high porosity of 75.27% and low mechanical strength of 1.29 MPa. While the dense membrane exhibits low porosity, but high liquid uptake about 300% and high mechanical strength of 10.47 MPa. Moreover, the PVFM based porous and dense polymer membranes absorb and swell liquid electrolyte to form stable gel polymer electrolytes (GPEs) with thermal stability. The GPE obtained from dense PVFM membrane shows ionic conductivity of 1.77×10^{-4} S cm^{-1} at room temperature and wide electrochemical window of 1.8–5.0 V (vs. Li/Li$^+$). Though the GPE formed by porous PVFM based membrane shows high ionic conductivity of 1.25×10^{-3} S cm^{-1}, the mechanical strength needs further improvement as polymer membrane for GPE through some techniques, such as doping inorganic particles,[12] and polymer blending method.[13]

In this paper, PEO blending has been chosen to improve mechanical properties of the PVFM based porous polymer membranes. PEO is extensively studied due to its strong complexing ability to many kinds of lithium salts and also unique structure for supporting fast ion transport.[14] However, its high crystalline phase concentration limits the room temperature conductivity of the electrolyte,[15] such as 10^{-5} S cm^{-1} for PEO-LiClO$_4$.[16] It has been reported that a certain content of PEO blending with PVDF-HFP matrix obviously improved its mechanical strength and ionic conductivity to 3.7 MPa and 1.3×10^{-4} S cm^{-1} at 30°C,[15] respectively. Furthermore, the blending of PEO with PVDF-LiClO$_4$ can also enhance mechanical stability of electrolyte membranes.[17] Therefore, PEO blending is a hopeful route to improve the mechanical properties of PVFM based membranes and ionic conductivity of their GPEs.

In this work, PVFM based porous membranes with PEO blending were prepared via the optimized phase inversion method. The PEO blending was found to improve the mechanical

strength of PVFM based membranes and conductivity of corresponding GPEs. Moreover, the Li/LiFePO$_4$ batteries using the blending GPEs showed good cyclic performance.

EXPERIMENTAL

Optimized Preparation Process of PEO/PVFM Blend Membrane and its GPEs

The mixtures of PVFM (MW: 70,000, Aldrich) and PEO (MW: 500,000, Aldrich) powders in ratios of 90 : 10, 80 : 20, 70 : 30 (w/w) were dissolved in N-methyl pyrrolidone (NMP, SCRC) at 70°C, since much more than 30 wt % PEO will lead to the transformation of membrane-forming mechanism from liquid–liquid phase separation to solid–liquid phase separation, which is too slow to precipitate freestanding membranes. Furthermore, the concentration of PVFM and PEO in NMP was controlled to be 10 wt %. Afterward, 4, 4′-diphenylmethane diisocyanate (MDI, Alfa Aesar), as PVFM crosslinking agent, was added into the above solution under stirring for 30 min at 75°C. The weight ratio of MDI and PVFM was fixed at 40%. The as obtained slurry was cast on a glass plate using a doctor blade with 30 μm gap and immersed in a coagulation bath which was composed of NMP and deionized water in a ratio of 1 : 20 (v/v) at 25°C. Unlike the preparation reported in our previous work,[11] the components of coagulation bath, i.e., the ratio of NMP as solvent and deionized water as nonsolvent was optimized to precipitate a membrane with improved morphology and performance. In the coagulation bath, the nonsolvent and the polymer solvent interdiffuse very soon due to the good interaction between NMP and H$_2$O. The instantaneous liquid–liquid phase separation of polymer solution took place consequently. The polymer-rich phase precipitated to form the membranes, while the polymer-poor phase, i.e., the H$_2$O-rich phase transformed into holes in the membranes. The total time for membranes precipitation in a coagulation bath was less than 2 min. And then the porous membrane was peeled off from the glass plate in the coagulation bath using a tweezer. Subsequently, the obtained membranes were washed with deionized water and the residual solution on the surface was absorbed by filter paper. Finally, the freestanding membranes with thickness of 70–95 μm were dried in vacuum at 25°C for 48 h and punched into disks of 16 mm in diameter. The corresponding GPEs were obtained by soaking PEO/PVFM blend membranes in liquid electrolyte (1M LiPF$_6$ in ethylene carbonate/diethyl carbonate/dimethyl carbonate (EC/DEC/DMC) = 1 : 1 : 1(v/v/v), BICR) until the polymer chains thoroughly swell. Moreover, a PVFM based GPE without PEO blending was also prepared for comparison.

Preparation of Electrode and Assembly of Cell

The cathode slurry was prepared by mixing LiFePO$_4$ active material powder, acetylene black and poly(vinylidene fluoride) (PVDF) binder in the ratio of 85 : 10 : 5 (w/w/w) in NMP solvent. Then, the slurry was coated on to the aluminum foil and dried at 120°C under vacuum for 24 h to prepare cathode electrode. Coin cells (CR2032) were assembled by sandwiching the PEO/PVFM blend GPEs between Li metal anodes and LiFePO$_4$ cathodes in an argon-filled glove box, in which the contents of water and oxygen are less than 0.5 ppm.

Characterizations and Measurements

Morphologies of PVFM based membranes with PEO blending were observed by field emission scanning electron microscopy (FESEM) (Carl Zeiss, SUPRA55, Germany). Crystallinity of blend membranes was characterized by X-ray diffraction (XRD) (Rigaku, TTRIII, Japan), from 10° to 60° at a scanning rate of 2° min^{-1}, and differential scanning calorimetry (DSC) (TA, Q2000) from 30 to 150°C at a heating rate of 5°C min^{-1}. Mechanical strength of membranes was measured on a tensile testing apparatus (INSTRON, 5567) at a tensile speed of 10 mm min^{-1}, using samples with size of 1 × 3 cm^2. Electrolyte uptake was evaluated by the weight change of membranes before and after immersed in liquid electrolyte at 25°C for 0.5 h. The electrolyte uptake value was calculated using the following eq. (1):

$$A(\%) = \frac{W_2 - W_1}{W_1} \times 100 \tag{1}$$

where W_1 and W_2 are the weights of the membrane and GPE, respectively.

Porosity of membranes was calculated according to eq. (2). The membranes were weighed firstly and then immersed in 1-butanol for 1 h. Finally the membranes were dried with filter paper and weighed again.

$$\phi(\%) = \frac{W_t - W_0}{\rho V} \times 100 \tag{2}$$

where W_t and W_0 are the weights of the wet and dry membrane, respectively. V is the apparent volume of the membrane, and ρ is the density of 1-butanol.

The density of membranes was determined by the ratio of their mass and apparent volume.

The ionic conductivity of GPE was measured by AC impedance spectroscopy using symmetrical cell SS/GPE/SS with potential amplitude of 5 mV from 100 kHz to 0.01 Hz. The ionic conductivity value was calculated according to eq. (3):

$$\sigma = \frac{l}{R \times S} \tag{3}$$

where l is the thickness of the GPE, S is the contact area between GPE and SS disc, R is the bulk electrolyte resistance. The electrochemical stability of PVFM/PEO blend GPE was measured by cyclic voltammetry measurements (Princeton Applied Research, VersaSTAT3) using a Li/GPE/SS cell with a stainless steel as working electrode and metallic lithium as counter and reference electrode at the scanning rate of 5 mV S^{-1} from 0 to 6 V (vs. Li/Li$^+$).

For the detail about the performance of GPE matching with LiFePO$_4$ electrode, galvanostatic charge, and discharge cycling tests of cells were conducted at 0.1C over a potential range of 2.5–4.25 V at room temperature (Jinnuo Wuhan Corp., LAND CT2001A).

RESULTS AND DISCUSSION

Scanning Electron Microscopy

The morphologies of membranes incorporating 0, 10, 20, 30% PEO are shown in Figure 1. Among them, Figure 1(a,d,g,j and b,e,h,k) exhibit the surface of underlying sides and free sides
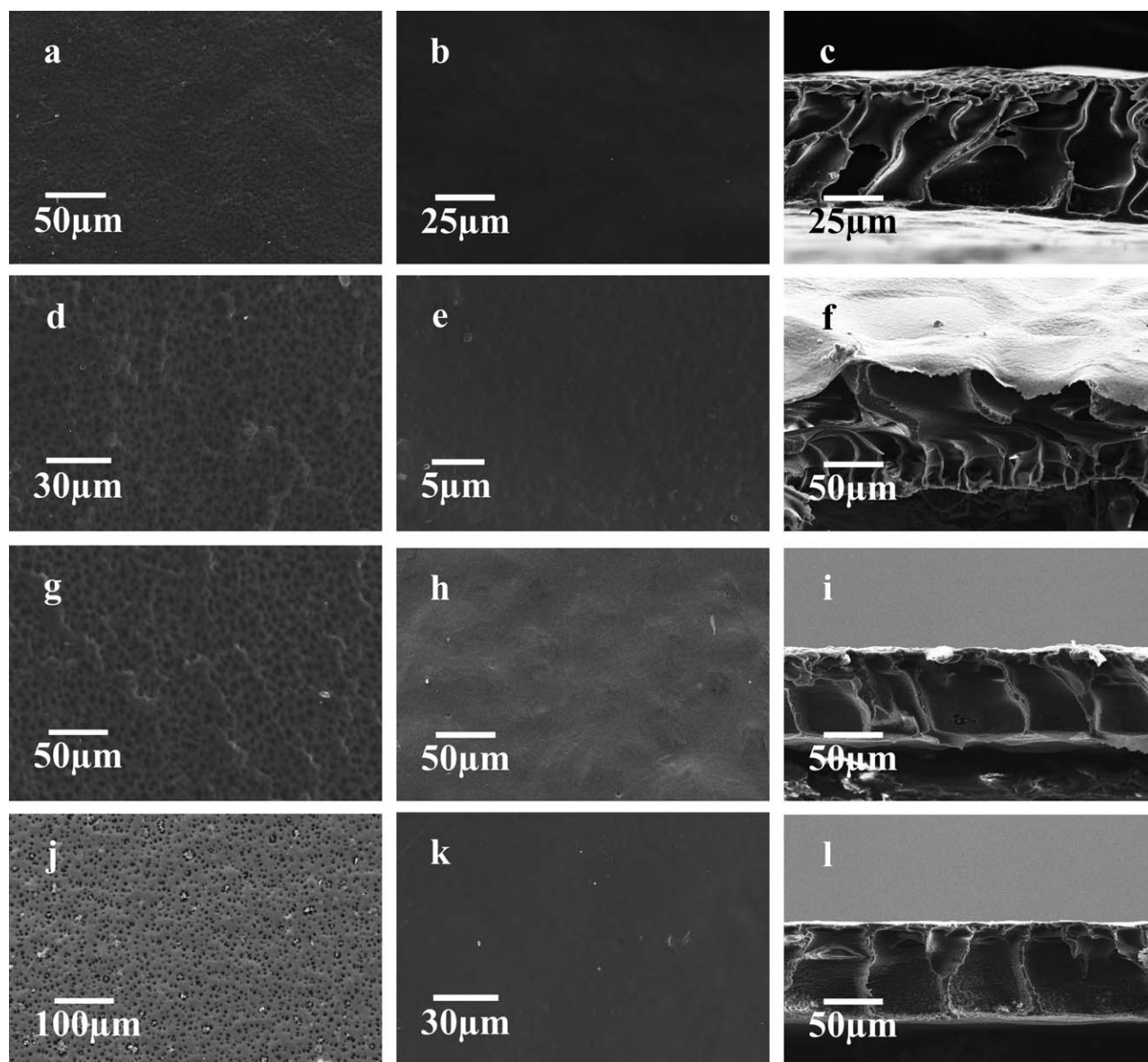
Figure 1. FESEM images of polymer membranes: (a–c) PVFM; (d–f) PVFM-10%PEO; (g–i) PVFM-20%PEO (j–l) PVFM-30% PEO.

contacting with coagulation bath, respectively. It can be seen that all membranes show dense morphology on the free sides but a number of cavities on the underlying surface, which ascribes to the faster diffusion of solvent NMP and higher concentration of polymer on the free sides, but the suppressed diffusion of solvent by membranes and lower concentration of polymer on the underlying sides. It is interesting to note from Figure 1(j) that a few particles are distributed on the surface of membrane incorporating 30% PEO, implying the phase separation of PEO and PVFM. The similar phenomenon can also be observed in the blend of poly(vinyl alcohol) (PVA) and PEO when the content of PEO is higher than 25 wt %,[18] which suggests that the mutual miscibility of PEO and PVA exists over only a small range of compositions.[19] In the same way, the phase separation phenomenon of membrane incorporating 30% PEO indicates that more than 30% PEO is incompatible with the PVFM. Finger-shaped holes can be observed from the cross sections of membranes shown in Figure 1(c,f,i,l). According to the ternary phase diagram of polymer–solvent–nonsolvent,[11] such porous structures are formed in poor phase nucleation metastable gap. Besides, the good interaction between solvent and nonsolvent in the coagulation bath contributes to fast diffusion of solvent and nonsolvent, leading to instantaneous liquid-liquid phase separation and resultant asymmetric membranes with thin skin and porous structure.[20] The size of finger-shaped holes observed from cross sections of membranes is increased with an increase of PEO content due to its good affinity for water, which accelerates the transfer of nonsolvent deionized water to polymer membranes. As a result, PVFM/PEO blend membranes show dense surface and large interconnecting holes in cross sections.
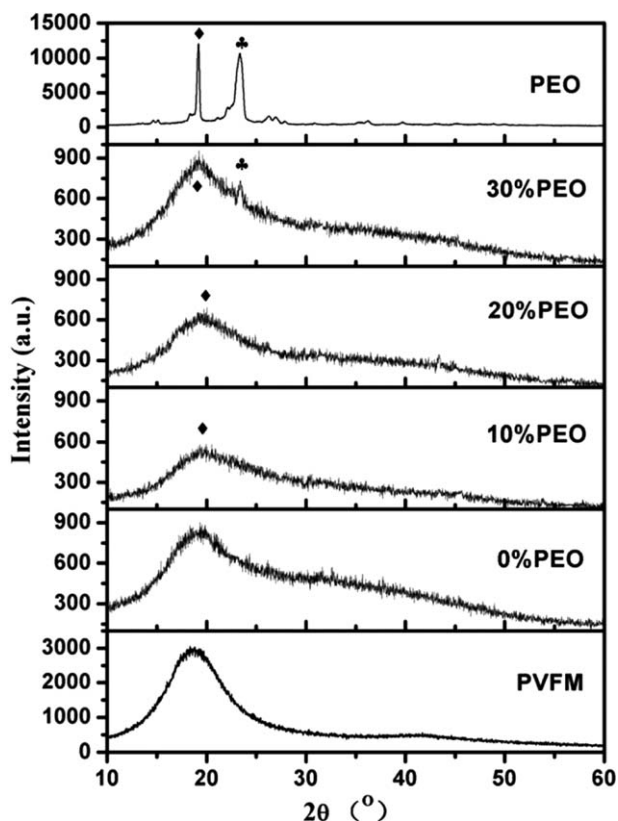
Figure 2. XRD patterns of PVFM, PEO (1-γ)PVFM-γPEO(γ = 0%, 10–30%) polymer membranes.

XRD Analysis

Figure 2 displays the XRD patterns of PVFM, PEO and membranes incorporating 0, 10, 20, 30% PEO. Both of PVFM and the membrane without PEO blending show one broad diffraction peak at 19.3°, indicating the semicrystalline nature of PVFM. As the integration of PEO, the intensity of diffraction peak at 19.3° is reduced at first and then increased with more PEO blending. Besides, the peak corresponding to PEO is absent at 23.4° until more PEO is blended with PVFM. The phenomenon indicates that a small amount of PEO is quite compatible with PVFM.[15] The PEO chains throughout PVFM network hinder the formation of hydrogen bonds between the unacetalized hydroxyls of PVFM and suppress the orderly arrangement of PVFM chains, which results in the reduced crystallinity of polymer matrix. As more PEO is blended, the phase separation of PEO and PVFM takes place as shown in SEM images, leading to the increased crystallinity of PEO. It can be concluded that a small amount of PEO blending can reduce the crystallinity of polymer matrix, while more than 30% PEO blending will increase the crystallinity of blending membranes on the contrary.

DSC Analysis

Figure 3 shows the DSC curves of PVFM, PEO, and polymer membranes containing PEO in different ratios. The PVFM shows one small endothermic peaks at 110°C, representing the glass transition of PVFM. When PVFM is crosslinked with MDI, it becomes more difficult for polymer chains to move. Therefore the temperature of glass transition becomes higher,
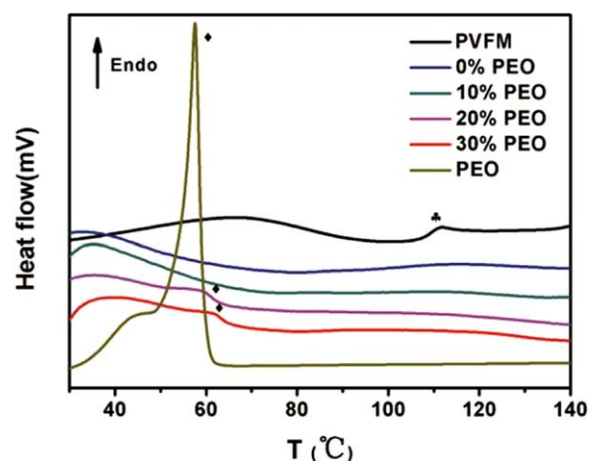
Figure 3. DSC curves of PVFM, PEO (1-γ)PVFM-γPEO(γ = 0%, 10–30%) polymer membranes. [Color figure can be viewed in the online issue, which is available at wileyonlinelibrary.com.]

and the PVFM based membrane without PEO exhibits no obvious endothermic peak between 30 and 140°C. With 10% PEO blending, the sample still shows undetectable peak in DSC curve, indicating the completely miscibility of PEO with PVFM, and the diminished crystalline structure of PEO.[15] However, a melting peak corresponding to PEO appears at 58.2°C, and a shift to a higher temperature of 60.6°C occurs with an increase of PEO content, which is consist with the literature report about the blend of PEO and poly(vinyl acetate) and implies the increase on crystallinity of PEO.[21]

Mechanical Property

Due to the crucial influence of membrane strength on battery safety, the tensile strength of membranes containing 0, 10, 20, 30% PEO is measured, as shown in Figure 4. The ultimate tensile strength and elongation-at break value of the membrane without PEO are 3.54 MPa and 9.68%, respectively. While the membrane with 10% PEO blending shows an increase in both ultimate tensile strength and elongation-at break value because of the soft chains in PEO and the good compatibility between
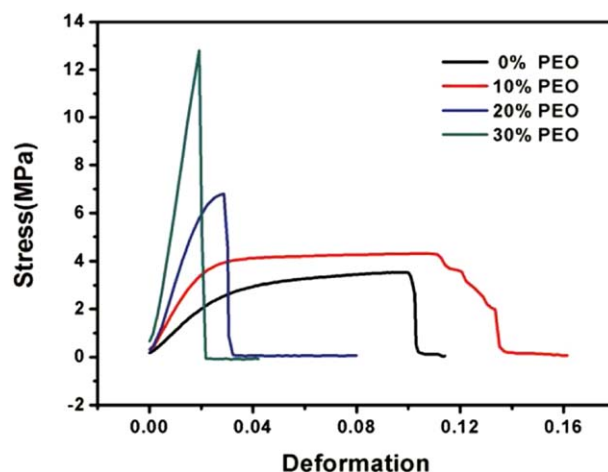
Figure 4. The stress–deformation curves of (1-γ)PVFM-γPEO (γ = 0, 10–30%) polymer membranes. [Color figure can be viewed in the online issue, which is available at wileyonlinelibrary.com.]

Table I. The Characterization on Physicochemical Properties of Membranes

Sample	Density (g cm^{-3})	Porosity (%)	Uptake (%)	Conductivity (×10^{-3} S cm^{-1})	Strength (MPa)
PVFM	0.32	57.4	387	0.42	3.54
PVFM-10%PEO	0.23	75.1	421	1.39	4.33
PVFM-20%PEO	0.25	75.4	413	1.83	6.80
PVFM-30%PEO	0.27	76.8	435	2.20	12.81

PVFM and PEO. As the content of PEO rises to 20, 30%, the ultimate tensile strength of membranes is enhanced continuously while the elongation-at break values decrease. When the weight ratio of PEO is 30 wt %, the mechanical strength of blending membrane achieved 12.81 MPa, which is even higher than the mechanical strength of PVFM based dense membrane.[12] The improvement of tensile strength can be attributed to the change of crystallization states in the PVFM/PEO blend membranes. The PEO chains throughout PVFM ones reduce the size of crystalline regions of PVFM, and lead to more uniformly distributed crystalline regions.[22] The increased crystalline regions, as physical joints in the polymer network, will bear the main stress and lead to the improvement of the mechanical properties of membranes. Additionally, the DSC and SEM results indicate that the crystallization of PEO is dominant with more than 20% PEO blending, and the size of PEO crystallites increased with the increase of PEO content. Since PEO crystallites absorb strain energy upon deformation through an unfolding of the crystalline lamellae or break up of crystalline segments,[23] the tensile strength of blend membranes can be increased. However, the PEO crystallites existing within PVFM chains will inhibit the orientation of PVFM chains under external tension, which leads to the decrease of elongation-at break values as PEO content is more than 20%.

Porosity, Electrolyte Uptake and Ionic Conductivity
Table I shows the porosity and electrolyte uptake values of PVFM based polymer membranes incorporating different ratios
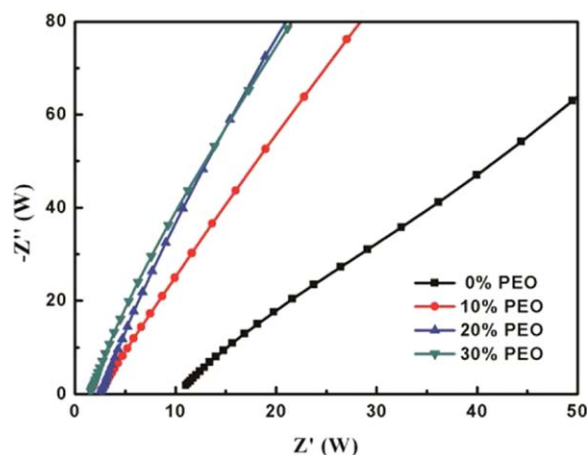
Figure 5. Nyquist plots of $(1-\gamma)$PVFM-γPEO ($\gamma = 0$, 10–30%) polymer electrolytes. [Color figure can be viewed in the online issue, which is available at wileyonlinelibrary.com.]

of PEO. It can be found that PVFM/PEO blend membranes exhibit higher porosity and higher electrolyte uptake than the membrane without PEO blending. The reason is that the interconnecting holes in cross sections of membranes become larger due to the addition of hydrophilic PEO, as detected in SEM images. Besides, the good compatibility between PEO and organic solvents in the liquid electrolyte also contributes to high electrolyte uptake.[24] The influence of PEO on porosity and electrolyte uptake agrees well with the literature reports.[25,26] What's interesting is that although the membranes show high electrolyte uptake, the change of thickness is less than 3%, which confirms the dimensional stability of PVFM/PEO blend membranes. To characterize the ionic conductivity of PVFM/PEO blend GPEs, membranes are immersed in liquid electrolyte to form GPEs, and AC impedance spectroscopy is tested as shown in Figure 5. The ionic conductivity of PVFM based GPE is a little bit lower than that of the liquid electrolyte itself due to the membrane resistance. For GPEs supported by porous membranes, there are usually two ionic conduction paths: one is the interconnected pores filled with liquid electrolyte, showing higher conductivity; the other one is the swollen polymer matrix as a slow conduction path. Therefore, when the porosity and electrolyte uptake increase with PEO blending, the ionic conductivity of PVFM/PEO blend GPEs is enhanced significantly. Moreover, the ionic conductivity of GPEs has a further improvement as the PEO content increases. The PVFM-30%PEO blend GPE shows high room temperature ionic conductivity of 2.20×10^{-3} S cm^{-1}, which is comparable with other excellent GPEs reported in recent years,[25–29] such as 2.30×10^{-3} S cm^{-1} for PVDF-TrFE/PEO blend polymer electrolyte.[27] It is worthy to note that there is no great difference between the electrolyte uptake values of PVFM/PEO blend membranes, indicating that electrolyte uptake is only one of the critical influences on conductivity of GPEs. Additionally, the good complexation between lithium salt and polymer such as PEO can increase the concentration of carrier ions in GPEs. Moreover, the soft chains of PEO and the large finger-shaped holes shown in cross sections of membranes are also beneficial to the transport of lithium ions in GPEs. Therefore, the increase of PEO content is favorable for the improvement of ionic conductivity, which is in accordance with literatures.[26]

Electrochemical Stability Window
To test the electrochemical stability windows of PVFM/PEO blend GPEs, the cyclic voltammetry curves of PVFM-30%PEO are measured at the scanning rate of 5 mV S^{-1} from 0 to 6 V (vs. Li/Li$^+$). As shown in Figure 6, a small peak at about 1.5 V can be seen during the reverse cathodic scan, which represents
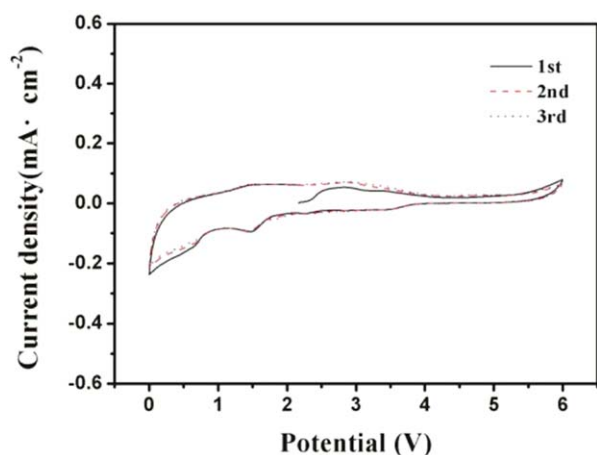
Figure 6. The cyclic voltammetry curve of PVFM-30%PEO based polymer electrolyte. [Color figure can be viewed in the online issue, which is available at wileyonlinelibrary.com.]

the reductive decomposition of EC in electrolyte solvent.[30,31] In the anodic scan, the oxidative decomposition of GPE occurs at about 5.7 V. The oxidative stability of PVFM/PEO blend GPE is higher than that of most GPEs, which reported to be 4.5–5.1 V (vs. Li/Li$^+$) in recent years.[32–35] Thus, PVFM-30%PEO blend GPE shows good electrochemical stability in the potential range from 1.9 to 5.7 V (vs. Li/Li$^+$), which is accessible to the application in lithium-ion batteries.

Cyclic Performance of Li/LiFePO$_4$ Cell

Figure 7 shows the initial charge and discharge performance of Li/LiFePO$_4$ cells using PVFM/PEO blend GPEs at 0.1C from 2.5 to 4.25 V at room temperature. The cells using PVFM based GPEs incorporating 10, 20, 30% PEO deliver discharge capacities of 134.2, 138.8, 140.8 mAh g^{-1} at the first cycle, respectively, which are higher than that of the cell using GPE without blending. The improved capacity ascribes to the higher conductivity of the blending GPEs. Figure 8 exhibits the cyclic performance of the Li/LiFePO$_4$ cells. The cells using PVFM based GPEs incorporating 10, 20, 30% PEO deliver the 40th discharge
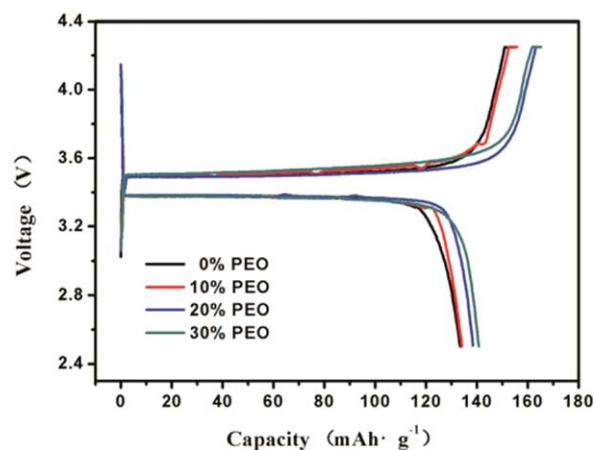
Figure 7. The initial charge–discharge curves of Li/GPEs/LiFePO$_4$ cells at 0.1C between 2.5 and 4.25 V. [Color figure can be viewed in the online issue, which is available at wileyonlinelibrary.com.]
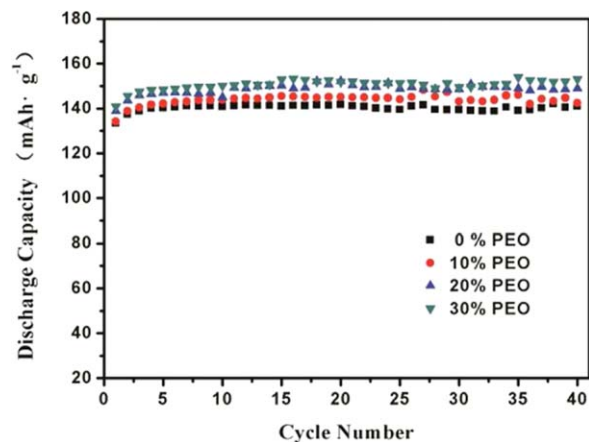
Figure 8. Cyclic stability of Li/GPEs/LiFePO$_4$ cells at 0.1C between 2.5 and 4.25 V. [Color figure can be viewed in the online issue, which is available at wileyonlinelibrary.com.]

capacity of 144.7, 148.5, 152 mAh g^{-1}, respectively, which confirms that the cells using the PVFM/PEO blend GPEs have good cyclic performance.

CONCLUSIONS

PVFM based polymer electrolyte membranes with PEO blending are prepared via phase inversion method. Compared with the membrane without blending, the membranes with the integration of PEO show higher porosity and higher electrolyte uptake, which is in favor of the increase of ionic conductivity of corresponding GPEs. Moreover, an obvious improvement of tensile strength from 3.54 to 12.81 MPa can be achieved by incorporating 30% PEO, though the extensibility of the membrane is decreased. When matching with LiFePO$_4$ electrode, the Li/LiFePO$_4$ cell using PVFM-30%PEO based GPE delivers an initial discharge capacity of 140.8 mAh g^{-1} and high cycling stability, indicating that PVFM-30%PEO based GPE is a very promising candidate for electrolyte applied in lithium-ion batteries.

REFERENCES

1. Liao, Y. H.; Sun, C. J.; Hu, S. J.; Li, W. S. *Electrochim. Acta* **2013**, *89*, 461.

2. Guan, H. Y.; Lian, F.; Xi, K.; Ren, Y.; Sun, J. L.; Kumar, R. V. *J. Power Sources.* **2014**, *245*, 95.

3. Stephan, A. M. *Eur. Polym. J.* **2006**, *42*, 21.

4. Gerbaldi, C.; Nair, J. R.; Meligrana, G.; Bongiovanni, R.; Bodoardo, S.; Penazzi, N. *J. Appl. Electrochem.* **2009**, *39*, 2199.

5. Kufian, M. Z.; Aziz, M. F.; Shukur, M. F.; Rahim, A. S.; Ariffin, N. E.; Shuhaimi, N. E. A.; Majid, S. R.; Yahya, R.; Arof, A. K. *Solid State Ionics* **2012**, *208*, 36.

6. Guilbert, A. A. Y.; Reynolds, L. X.; Bruno, A.; Maclachlan, A.; King, S. P.; Faist, M. A.; Pires, E.; Macdonald, J. E.; Stingelin, N. S.; Haque, A.; Nelson, J. *ACS Nano* **2012**, *6*, 3868.

7. Raghavan, P.; Manuel, J.; Zhao, X. H.; Kim, D. S.; Ahn, J. H.; Nah, C. *J. Power Sources* **2011**, *196*, 6742.

8. Kim, C. H.; Kim, H. T.; Park, J. K.; Moon, S. I.; Yoon, M. S. *J. Polym. Sci., Part B: Polym. Phys.* **1996**, *34*, 2709.

9. Saunier, J.; Alloin, F.; Sanchez, J. Y.; Barriere, B. *J. Polym. Sci., Part B: Polym. Phys.* **2004**, *42*, 532.

10. Elmér, A. M.; Jannasch, P. *J Polym. Sci., Part B: Polym. Phys.* **2007**, *45*, 79.

11. Ren, Y.; Lian, F.; Wen, Y.; Guan, H. Y. *Polymer* **2013**, *54*, 4807.

12. Wen, Y.; Lian, F.; Ren, Y.; Guan, H. Y. *J. Polym. Sci. Part B: Polym. Phys.* **2014**, *52*, 572.

13. Kim, S. H.; Choi, J. K.; Bae, Y. C. *J. Appl. Polym. Sci.* **2001**, *81*, 948.

14. Fan, L. Z.; Nan, C. W.; Zhao, S. J. *Solid State Ionics* **2003**, *164*, 81.

15. Fan, L. Z.; Dang, Z. M.; Nan, C. W.; Li, M. *Electrochim Acta* **2002**, *48*, 205.

16. Michael, M. S.; Jacob, M. M. E.; Prabaharan, S. R. S.; Prabaharan, S. *Solid State Ionics* **1997**, *98*, 167.

17. Jacob, M. M. E.; Prabaharan, S. R. S.; Radhakrishna, S. *Solid State Ionics* **1997**, *104*, 267.

18. Sawatari, C.; Kondo, T. *Macromolecules* **1999**, *32*, 1949.

19. Mishra, R.; Rao, K. J. *Eur. Polym. J.* **1999**, *35*, 1883.

20. Xu, Y. Y.; Xu, Z. K. Polymer Membrane Materials; Ding, S. L.; Zhou, H., Eds.; Chemical Industry Press: Beijing, **2005**; Chapter 2, pp 19–73.

21. Wu, W. B.; Chiu, W. Y.; Liau, W. B. *J. Appl. Polym. Sci.* **1997**, *64*, 411.

22. Ding, W.; Du, M.; Zheng, Q. *J Zhejiang Univ.* **2013**, *47*, 1109.

23. Korley, L. T. J.; Pate, B. D.; Thomas, E. L.; Hammond, P. T. *Polymer* **2006**, *47*, 3073.

24. Kim, D. W.; Ko, J. M.; Chun, J. H.; Kim, S. H.; Park, J. K. *Electrochem. Commun.* **2001**, *3*, 535.

25. Li, H.; Zhang, H.; Liang, Z. Y.; Chen, Y. M.; Zhu, B. K.; Zhu, L. P. *Electrochim. Acta* **2014**, *116*, 413.

26. Xi, J.; Qiu, X. P.; Li, J.; Tang, X. Z.; Zhu, W. T.; Chen, L. Q. *J. Power Sources* **2006**, *157*, 501.

27. Costa, C. M.; Gomez Ribelles, J. L.; Lancerous-Mendez, S.; Appetecchi, G. B.; Scrosati, B. *J. Power Sources* **2014**, *245*, 779.

28. Idris, N. H.; Rahman, M. M.; Wang, J. Z.; Wang, J. Z. *J. Power Sources.* **2012**, *201*, 294.

29. Prasanth, R.; Shubha, N.; Hng, H. H.; Srinivasan, M. *J. Power Sources.* **2014**, *245*, 283.

30. Zhang, X.; Kostecki, R.; Richardson, T. J.; Pugh, J. K.; P. N. Ross. *J. Electrochem. Soc.* **2001**, *148*, A1341.

31. Bridel, J. S.; Grugeon, S.; Laruelle, S.; Hassoun, J.; Reale, P.; Scrosati, B.; Tarason, J. M. *J. Power Sources.* **2010**, *195*, 2036.

32. Wang, X.; Gong, C.; He, D.; Xue, Z.; Chen, C.; Liao, Y.; Xie, X. *J. Membr. Sci.* **2014**, *454*, 298.

33. Cheng, Q.; Cui, Z.; Li, J.; Qin, S.; Yan, F.; Li, J. *J. Power Sources.* **2014**, *266*, 401.

34. Zhang, H.; Ma, X.; Lin, C.; Zhu, B. *RSC Adv.* **2014**, *4*, 33713.

35. Zhou, L.; Wu, N.; Cao, Q.; Jing, B.; Wang, X.; Wang, Q.; Kuang, H. *Solid State Ionics* **2013**, *249–250*, 93.